

Ginkgo leaf cuticle chemistry across changing pCO₂ regimes

--Manuscript Draft--

Manuscript Number:							
Full Title:	Ginkgo leaf cuticle chemistry across changing pCO ₂ regimes						
Article Type:	Research Paper						
Corresponding Author:	Phillip Jardine, Ph.D. Westfälische Wilhelms-Universität Münster GERMANY						
Corresponding Author Secondary Information:							
Corresponding Author's Institution:	Westfälische Wilhelms-Universität Münster						
Corresponding Author's Secondary Institution:							
First Author:	Phillip Jardine, Ph.D.						
First Author Secondary Information:							
Order of Authors:	Phillip Jardine, Ph.D. Matthew Kent Wesley T. Fraser Barry H. Lomax						
Order of Authors Secondary Information:							
Funding Information:	<table border="1"> <tr> <td>Palaeontological Association (PA-RG201802)</td> <td>Dr Phillip Jardine</td> </tr> <tr> <td>Natural Environment Research Council (NE/R001324/1)</td> <td>Dr Barry H. Lomax</td> </tr> <tr> <td>Natural Environment Research Council (NE/P013724/1)</td> <td>Dr Wesley T. Fraser</td> </tr> </table>	Palaeontological Association (PA-RG201802)	Dr Phillip Jardine	Natural Environment Research Council (NE/R001324/1)	Dr Barry H. Lomax	Natural Environment Research Council (NE/P013724/1)	Dr Wesley T. Fraser
Palaeontological Association (PA-RG201802)	Dr Phillip Jardine						
Natural Environment Research Council (NE/R001324/1)	Dr Barry H. Lomax						
Natural Environment Research Council (NE/P013724/1)	Dr Wesley T. Fraser						
Abstract:	<p>Cuticles have been a key part of palaeobotanical research since the mid-19th Century. Recently, cuticular research has moved beyond morphological traits to incorporate the chemical signature of modern and fossil cuticles, with the aim of using this as a taxonomic and classification tool. For this approach to work cuticle chemistry would have to maintain a strong taxonomic signal, with a limited input from the ambient environment in which the plant grew. Here, we use attenuated total reflectance Fourier Transform infrared (ATR-FTIR) spectroscopy to analyse leaf cuticles from <i>Ginkgo biloba</i> plants grown in experimentally enhanced CO₂ conditions, to test for the impact of changing CO₂ regimes on cuticle chemistry. We find limited evidence for an impact of CO₂ on the chemical signature of <i>Ginkgo</i> cuticles, which supports the use of chemotaxonomy for plant cuticular remains across geological timescales.</p>						
Suggested Reviewers:	<p>Vivi Vajda vivi.vajda@nrm.se Professor Vajda has published on modern and fossil cuticle chemotaxonomy</p> <p>Margaret Collinson M.Collinson@rhul.ac.uk Professor Collinson has researched plant cuticle chemistry and diagenesis</p> <p>Boris Zimmermann boris.zimmermann@nmbu.no Dr Zimmermann has researched FTIR-based chemotaxonomy of pollen and spores</p>						



[Click here to view linked References](#)

1 ***Ginkgo* leaf cuticle chemistry across changing $p\text{CO}_2$ regimes**

2
3
4
5 3 Phillip E. Jardine¹, Matthew Kent², Wesley T. Fraser³, and Barry H. Lomax²
6
7 4

8
9
10 5 ¹Institute of Geology and Palaeontology, University of Münster, 48149 Münster, Germany.

11 6 jardine@uni-muenster.de
12
13

14 7 ²Agriculture and Environmental Science, University of Nottingham, Sutton Bonington
15

16 8 Campus, Leicestershire, LE12 5RD, UK. Matthew.Kent@nottingham.ac.uk,
17
18

19 9 Barry.Lomax@nottingham.ac.uk
20

21 10 ³Geography, Department of Social Sciences, Oxford Brookes University, Oxford OX3 0BP,
22
23

24 11 UK. wfraser@brookes.ac.uk
25
26
27 12
28
29 13
30
31
32
33
34
35
36
37
38
39
40
41
42
43
44
45
46
47
48
49
50
51
52
53
54
55
56
57
58
59
60
61
62
63
64
65

14 **Abstract**

15 Cuticles have been a key part of palaeobotanical research since the mid-19th Century.
16 Recently, cuticular research has moved beyond morphological traits to incorporate the
17 chemical signature of modern and fossil cuticles, with the aim of using this as a taxonomic
18 and classification tool. For this approach to work cuticle chemistry would have to maintain a
19 strong taxonomic signal, with a limited input from the ambient environment in which the
20 plant grew. Here, we use attenuated total reflectance Fourier Transform infrared (ATR-FTIR)
21 spectroscopy to analyse leaf cuticles from *Ginkgo biloba* plants grown in experimentally
22 enhanced CO₂ conditions, to test for the impact of changing CO₂ regimes on cuticle
23 chemistry. We find limited evidence for an impact of CO₂ on the chemical signature of
24 *Ginkgo* cuticles, which supports the use of chemotaxonomy for plant cuticular remains across
25 geological timescales.
26
27
28

29
30
31 **Keywords** cuticle, *Ginkgo*, CO₂, ATR-FTIR, chemotaxonomy, geochemistry
32
33
34
35
36
37
38
39
40
41
42
43
44
45
46
47
48
49
50
51
52
53
54
55
56
57
58
59
60
61
62
63
64
65

29 **Introduction**

30 The plant cuticle is a key evolutionary innovation that enabled plants to colonise
31 subaerial environments in the early Palaeozoic (Domínguez et al. 2011; Renault et al. 2017;
32 Salminen et al. 2018). It is a waxy and waterproof membrane that covers the outer surface of
33 the green parts of plants, preventing desiccation and regulating gas exchange, as well as
34 providing structural support and protection from ultraviolet (UV) irradiance, herbivory, and
35 infection (Kerp 1990; Domínguez et al. 2011; Heredia-Guerrero et al. 2014; Dominguez et al.
36 2017). Cuticles consist of an insoluble aliphatic matrix comprising cutin (a long chain
37 polymer composed of esterified fatty acids), cutan (an ether-linked hydrocarbon polymer), or
38 a mixture of the two. Distributed through the matrix are soluble waxes and phenolic
39 compounds; waxes also occur on the outer surface of the matrix. The inner part of the matrix,
40 which connects with the epidermal cells, contains a high concentration of polysaccharides
41 (Domínguez et al. 2011; Heredia-Guerrero et al. 2014; Dominguez et al. 2017).

42
43 Plant cuticles have been investigated and utilised by palaeobotanists for over 170
44 years (Kerp 1990). Cuticles have a high preservation potential, retaining anatomical details
45 such as epidermal cell morphologies and stomata distributions (Kerp 1990), and have
46 therefore been used in a variety of applications, including fossil plant taxonomy and
47 determining the botanical affinities of disparate plant organs (Kerp 1990; Kerp et al. 2006;
48 Abu Hamad et al. 2008; Bomfleur et al. 2013; Abu Hamad et al. 2017), reconstructing
49 atmospheric $p\text{CO}_2$ from stomatal densities or associated indices (Woodward 1987;
50 McElwain and Chaloner 1995; Lomax and Fraser 2015; McElwain and Steinthorsdottir
51 2017), and reconstructing genome size based on guard cell length (Lomax et al. 2014).
52 Recently, Steinthorsdottir et al. (2018) suggested that morphological changes in the cuticle

1
2 53 surface, such as stomatal complex distortion and disorganised cell arrangements, could be a
3 54 potential proxy for volcanic SO₂ emissions.
4
5 55

6
7 56 In addition to morphology-based analyses of cuticles, other studies have focused on
8
9 57 utilising cuticle chemistry. One area of interest has been generating carbon isotope data from
10
11 58 dispersed cuticles and thereby reconstructing carbon cycle dynamics (e.g. Richey et al. 2018),
12
13 59 and by combining with isotopic estimates of the $\delta^{13}\text{C}$ of the atmosphere it may be possible to
14
15 60 determine changes in water use efficiency (Diefendorf et al. 2010). Molecular analysis (e.g.
16
17 61 by pyrolysis-gas chromatography-mass spectrometry) of cuticle has also provided a wealth of
18
19 62 information, including the chemical composition of cuticles, the distribution of cutin and
20
21 63 cutan among plant taxa, and the fate of these biopolymers in the geological record (Tegelaar
22
23 64 et al. 1993; Mösle et al. 1997; Mösle et al. 1998; Zodrow and Mastalerz 2001; Mösle et al.
24
25 65 2002; Zodrow and Mastalerz 2002; Gupta et al. 2007a; Gupta et al. 2007b; Zodrow et al.
26
27 66 2012a; Zodrow et al. 2012b; see also Gupta 2014 for review).
28
29
30
31
32
33
34 67

35
36 68 Vibrational spectroscopic techniques such as Fourier transform infrared (FTIR) and
37
38 69 Raman spectroscopy have also been used to analyse cuticle chemistry, because they have the
39
40 70 advantages of being non-destructive, efficient and able to analyse very small sample
41
42 71 quantities (Heredia-Guerrero et al. 2014; Olcott Marshall and Marshall 2014). These
43
44 72 approaches have been employed in both modern and fossil settings, with the aims of
45
46 73 understanding cuticle chemistry and its response to environmental change and ontogenetic
47
48 74 development (Villena et al. 2000; Ribeiro da Luz 2006; Dominguez et al. 2012),
49
50 75 diagenesis/fossilisation processes and the characterisation of organic matter in the geological
51
52 76 record (Lyons et al. 1995; Zodrow et al. 2000; Zodrow and Mastalerz 2002; D'Angelo 2006;
53
54 77 Zodrow et al. 2009; Zodrow and Mastalerz 2009; D'Angelo et al. 2010; D'Angelo et al.
55
56
57
58
59
60
61
62
63
64
65

1
2
3
4
5
6
7
8
9
10
11
12
13
14
15
16
17
18
19
20
21
22
23
24
25
26
27
28
29
30
31
32
33
34
35
36
37
38
39
40
41
42
43
44
45
46
47
48
49
50
51
52
53
54
55
56
57
58
59
60
61
62
63
64
65

78 2011; Zodrow et al. 2012a; Zodrow et al. 2012b; D'Angelo and Zodrow 2015; Zodrow et al.
79 2016), and the taxonomic identification of plants using their chemical signature (termed
80 chemotaxonomy) (Zodrow and Mastalerz 2001, 2002; D'Angelo 2006; D'Angelo et al. 2010;
81 D'Angelo and Zodrow 2015; Vajda et al. 2017). Cuticle chemistry has been shown to contain
82 a phylogenetic signal that is preserved in fossil material, leading to the possibility of
83 classifying fragmentary or otherwise problematic cuticular remains (Vajda et al. 2017).
84 Parallel developments have been made in pollen and spore research (Pappas et al. 2003;
85 Dell'Anna et al. 2009; Zimmermann and Kohler 2014; Julier et al. 2016; Zimmermann et al.
86 2016), suggesting that FTIR or Raman based chemotaxonomy may have much to offer for
87 palaeobotanical and palynological investigations.

88
89 For cuticle chemistry to be successfully used for chemotaxonomy, it is critical to
90 understand the other possible controls on the chemical signature that may bias or obscure any
91 taxonomic or phylogenetic signal. Changing ambient UV-B levels are expected to drive
92 variations in the concentrations of phenolic compounds, for example, since these form the
93 UV-B absorbing compounds (UACs) in the plant cuticle (Blokker et al. 2006; Rozema et al.
94 2009). Such a relationship has been demonstrated in *Polylepis tarapacana* in the Bolivian
95 Andes (Gonzalez et al. 2007) and *Fagus sylvatica* from the Hunsrück region of Germany
96 (Neitzke and Therburg 2003), where leaf UAC concentrations increased with increased UV-
97 B at higher altitudes (although it should be noted that these findings relate to bulk leaf tissue,
98 rather than isolated cuticles). Over longer geological timescales, atmospheric CO₂
99 concentration may be a more important parameter, because it has varied from ~200 to ~2000
100 ppm since the appearance of the earliest plant cuticles >400 Ma (McElwain and
101 Steinthorsdottir 2017) (Fig. 1); however, the impacts of changes in atmospheric CO₂
102 concentrations on cuticle chemistry are currently not well understood. From a carbon

103 economic perspective, in a high CO₂ world such as the early Mesozoic biomolecules with a
104 high carbon content and thus metabolite cost would be cheaper to construct due to an increase
105 in substrate, suggesting a response to changes in CO₂ is expected. While a strong cuticular
106 chemical response to CO₂ would possibly limit the use of chemotaxonomy across long
107 timescales, it could open up the possibility of new indicators of palaeo-CO₂ concentrations.

108
109 Here we investigate the effect of different CO₂ regimes on *Ginkgo biloba* leaf cuticle
110 chemistry. *Ginkgo* is a particularly relevant taxon for addressing this uncertainty because of
111 its longevity: *Ginkgo* first appeared in the early Mesozoic, and Ginkgoales in the late
112 Palaeozoic (Zhiyan and Xiangwu 2006), and this group has therefore existed across a wide
113 range of CO₂ regimes (Fig. 1). Modern and fossil *Ginkgo* cuticles have also been the subject
114 of past chemical research, meaning that the overall chemistry and diagenetic changes are
115 broadly understood (Mösle et al. 1997, 1998).

116 117 **Methods**

118 The leaf cuticles analysed in this study were taken from *Ginkgo biloba* plants
119 experimentally grown under elevated CO₂ conditions, the full details of which can be found
120 in Gill et al. (2018). Briefly, *Ginkgo biloba* seedlings were grown for 6 months in walk-in
121 growth room chambers (UNIGRO, UK) at CO₂ concentrations of 400, 1200 and 2000 ppm.
122 Levington M3 was used as a potting medium, and the plants were kept well-watered during
123 the growth period. The plants were grown in a simulated day/night program with 10 hours of
124 light (300 μmol/m²/s) per day, a night high temperature of 17°C and a daytime peak
125 temperature of 22°C. Relative humidity was held at 70%. After 6 months, leaves were
126 harvested from the plants and dried at 60°C. For our FTIR analyses we generated data for 2

127 plants per CO₂ treatment, using pre-cut leaf discs from 3 leaves per plant, resulting in a total
128 of 18 leaves analysed.

129
130 IR spectra were generated using a Cary 670 FTIR spectrometer integrated with a Cary
131 620 FTIR microscope (Agilent, Santa Clara, CA, USA). The FTIR microscope was fitted
132 with a 64x64 pixel focal plane array (FPA) detector, and a 15x Vis/IR objective at high
133 magnification to which a Germanium crystal micro-attenuated total reflectance (ATR) was
134 fitted, achieving a resolution of 1.1 μm per pixel (each pixel results in one IR spectrum, so
135 that each measurement yields an array of $64 \times 64 = 4096$ spectra). Three replicate
136 measurements per leaf disc (abaxial side) were collected at 64 scans per measurement and a
137 resolution of 8. Background spectra were collected prior to each set of replicates and
138 automatically removed from the sample spectra. While we focused on the abaxial surface, the
139 adaxial surface from one leaf disc per CO₂ treatment was also analysed, again with three
140 replicate measurements, to compare chemical signals between the leaf sides.

141
142 The Cary 620 FTIR microscope allows a live view of the FPA detector which
143 maximises the potential of good contact between the ATR crystal and the sample. At a micro-
144 scale, the leaf surface was irregular and contact between the ATR Germanium crystal and the
145 leaf was not uniform, resulting in variable quality of spectra across the measurement array.
146 For each measurement, spectra were therefore extracted from those pixels where the height
147 (=absorbance value) of the 1167 cm^{-1} peak exceeded 15% of the maximum 1167 cm^{-1} peak
148 height within the array. The 1167 cm^{-1} peak was chosen because it is clearly present in all
149 spectra (Figs. 2 and 3), and 15% of the maximum peak height was used as a threshold
150 because it provides a reasonable trade-off between obtaining high quality spectra and
151 incorporating a sufficient number of spectra in each measurement. The mean of the extracted

152 spectra was then calculated to provide one spectrum per replicate measurement, and three
153 spectra per leaf disc.

154
155 Some spectra showed strong distortion in the higher wavenumbers, and so all were
156 limited to $<3100\text{ cm}^{-1}$ prior to analysis. Baseline curvature was removed with a 4th order
157 polynomial baseline, and the corrected spectra z-score standardised (i.e. the mean was
158 subtracted and the spectra divided by the standard deviation, resulting with each spectrum
159 having a mean of zero and a standard deviation of one). Peak assignment was carried out with
160 reference to the published literature (Ramirez et al. 1992; Heredia-Guerrero et al. 2014).

161
162 Spectral changes across the CO₂ treatments were analysed in two ways: with Principal
163 Components Analysis (PCA) and by measuring the heights of selected peaks. PCA is an
164 exploratory multivariate technique that partitions data into axes of maximal variation
165 (principal components), allowing complex multivariate data to be viewed in a limited number
166 of dimensions. Some spectra showed distortion in the 2800 to 1800 cm^{-1} range, even after the
167 4th order polynomial baseline correction, and this was found to swamp the PCA analysis such
168 that it dominated the first axis (the principal component that explains most variation in the
169 data). Prior to PCA the raw spectra were therefore limited to $<1800\text{ cm}^{-1}$, baseline corrected
170 with a linear baseline, and z-score transformed. Processing the spectra with Savitzky-Golay
171 smoothing and taking derivatives did not substantially alter the distribution of samples in
172 ordination space, so we limited our analyses to unprocessed spectra to make interpretation of
173 loadings plots more straightforward.

174
175 Peak height measurements were similar when taken from both the $<3100\text{ cm}^{-1}$ spectra
176 with a 4th order polynomial baseline correction and $<1800\text{ cm}^{-1}$ spectra with a linear baseline

177 correction. We therefore used the $<3100\text{ cm}^{-1}$ spectra, so as to include the aliphatic peaks at
178 2920 and 2850 cm^{-1} . Peaks were selected so that changes across the different components of
179 the cuticle (i.e. cutin, waxes, phenolic compounds, and polysaccharides; previous research
180 has shown that *Ginkgo* cuticles contain no cutan (Mösle et al. 1997)) could be detected, and
181 peak height was measured as the maximum absorbance value within a predetermined range
182 (see Table 1 for details). All data analysis was carried out in R v.3.4.2 (R Core Team 2017)
183 using the packages baseline v.1.2-1 (Liland and Mevik 2015) and prosopctr v.0.1.3 (Stevens
184 and Ramirez-Lopez 2013). IR spectral data are provided in the supplementary information.

185

186 Results

187 ATR-FTIR spectra of the *Ginkgo* cuticles reveals many of the same peaks that have
188 been previously identified in other studies (Fig. 2). Specifically, peaks relating to aliphatic
189 compounds in cutin and waxes are located at 2920 cm^{-1} (CH_2 asymmetric stretching), 2850
190 cm^{-1} (CH_2 symmetric stretching), 1460 cm^{-1} and 1370 cm^{-1} (both CH_2 bending), peaks related
191 to ester vibrations in cutin are located at 1710 cm^{-1} (with shoulders at 1730 cm^{-1} and 1685
192 cm^{-1} ; C=O stretching), 1167 cm^{-1} and 1104 cm^{-1} (both C-O-C stretching), peaks related to
193 phenolic compounds are located at 1605 cm^{-1} (C-C stretching) and 1515 cm^{-1} (C-C stretching
194 conjugated with C=C), and peaks related to polysaccharides are located at 1245 cm^{-1} (OH
195 bending; this peak may also represent cutin) and 1020 cm^{-1} (C-O stretching). Most of the
196 same peaks are present in both the abaxial and adaxial cuticles, although the abaxial cuticles
197 have a relatively higher 1167 cm^{-1} ester peak and 1605 cm^{-1} aromatic peak, related to cutin
198 and phenolic compounds, respectively, and the adaxial cuticles have a pronounced 1720 cm^{-1}
199 ester peak and a relatively higher 1245 cm^{-1} hydroxyl peak, related to cutin and
200 polysaccharides or cutin, respectively (Fig. 3). The spectra do not show any obvious
201 differences across CO_2 treatments (Fig. 3).

202

1
2 203 A PCA of the spectral data shows the major variability in the dataset is partitioned
3
4
5 204 between the abaxial and adaxial cuticles, which are separated on axis 1 of the ordination, and
6
7 205 to some extent on axis 4 (Fig. 4). There are no clear groupings associated with CO₂ treatment
8
9
10 206 on any of the first four PCA axes, which together account for >90% of the variation in the
11
12 207 data. Loadings plots show that PCA axis 1 is driven by variations in the 1720 and 1245 cm⁻¹
13
14 208 peaks (positive relationship; these peaks are higher in the adaxial cuticles) and peaks between
15
16
17 209 1000 and 1100 cm⁻¹ (negative relationship). Axes 2 and 3 are primarily driven by variations
18
19 210 around 1700 cm⁻¹, while the distribution of samples on axis 4 is underpinned by variations in
20
21
22 211 the height of the 1167 cm⁻¹ peak, which again differs between the abaxial and adaxial
23
24 212 cuticles. This lack of a chemical change with increasing CO₂ is also shown in the 2nd
25
26 213 derivative of Savitzky-Golay smoothed spectra, and when only the abaxial cuticles are
27
28
29 214 ordinated (Fig. S1).

30
31 215

32
33
34 216 Analysis of peak heights suggests that there are limited consistent changes with CO₂
35
36 217 level (Fig. 5). One possible exception is the 1460 cm⁻¹ aliphatic peak, and in the adaxial
37
38
39 218 cuticles the 2920 and 2850 cm⁻¹ aliphatic peaks as well, which decline in height with
40
41 219 increasing CO₂. However, the change in the height of the 1460 cm⁻¹ peak is less obvious in
42
43
44 220 the <1800 cm⁻¹ spectra (Fig. S2), so this may be an artefact of the baseline correction in the
45
46 221 <3100 cm⁻¹ spectra.

47
48 222

50 51 223 **Discussion and conclusions**

52
53 224 Our results suggest that, at least in terms of broad scale chemical signals, changes in
54
55
56 225 atmospheric CO₂ concentrations only have a limited impact upon *Ginkgo* cuticle chemistry.

57
58 226 While this is not an encouraging outcome for developing new CO₂ proxies from FTIR

227 analysis of cuticles, it does suggest that any taxonomic signature present in fossil cuticles will
228 be robust to the ambient CO₂ concentration that the plant was growing in. Chemotaxonomic
229 approaches should therefore be applicable across varying CO₂ regimes. There is some
230 evidence for a decrease in the aliphatic peaks, which may relate to decreases in the
231 epicuticular or intracuticular waxes with increasing CO₂, although these are most obvious
232 with the adaxial spectra where the quantity of data is limited. A more obvious driver of
233 differences in chemistry was the difference between abaxial and adaxial cuticles, related to
234 differences in the cutin matrix and intracuticular phenolic compounds. These findings require
235 investigation with a larger dataset, incorporating more taxa and increased replication of both
236 abaxial and adaxial surfaces.

237
238 It will also be necessary to confirm the generality of these results using processed and
239 isolated cuticles where non-fossilisable components have been removed (e.g. Möhle et al.
240 1998). This will allow for a better comparison with fossil material, including building
241 chemical libraries of modern taxa that can be used to classify fossil specimens. However, the
242 recognition of peaks from previous studies of chemically and mechanically isolated cuticles
243 (e.g. Heredia-Guerrero et al. 2014) in our IR spectra demonstrates that working with the outer
244 surfaces of intact leaves can provide generally applicable information on the drivers of cuticle
245 chemical variability. ATR analysis of unprocessed leaf surfaces provides a rapid means of
246 assessing cuticle chemistry, with field measurements a possibility if a handheld ATR is used
247 (Ribeiro da Luz 2006).

248
249 Our small-scale study does not rule out a possible influence of CO₂ on cuticle
250 chemistry, but it does suggest that the effects are likely to be subtle. In addition to increasing
251 the number of taxa, plants and leaves analysed, spectral deconvolution and curve fitting

252 approaches (e.g. Zodrow and Mastalerz 2001; Depciuch et al. 2018) may help to reveal small
1
2 253 differences across CO₂ treatments that might not be detected with the broad scale methods
3
4
5 254 used here. In particular, changes in the carbon isotope composition of the cuticle with
6
7 255 increasing CO₂ concentrations may cause small shifts in peak positions (Esler et al. 2000),
8
9
10 256 which if consistent across individuals and taxa may be detectable with careful analysis.

11
12 257
13
14 258 In addition to CO₂, other possible influencing factors will need to be tested for before
15
16
17 259 cuticle chemistry can be confidently used as a taxonomic tool across palaeoenvironments and
18
19 260 time periods. Of critical importance will be determining how well chemical signals from
20
21
22 261 external environmental conditions preserve in fossil cuticles. As already noted, one likely
23
24 262 driver of cuticle chemical change will be variations in UV-B irradiance, which are known to
25
26
27 263 control concentrations of UV-B absorbing compounds (UACs) in plant tissues (Rozema et al.
28
29 264 1999; Neitzke and Therburg 2003; Gonzalez et al. 2007; Rozema et al. 2009). The
30
31
32 265 concentration of UACs in pollen and spore walls has been shown to covary with ambient
33
34 266 UV-B flux, and this relationship has been consistently demonstrated across a range of taxa
35
36 267 and time periods (Rozema et al. 1999; Rozema et al. 2001a; Rozema et al. 2001b; Blokker et
37
38
39 268 al. 2005; Blokker et al. 2006; Watson et al. 2007; Lomax et al. 2008; Rozema et al. 2009;
40
41 269 Fraser et al. 2011; Willis et al. 2011; Lomax et al. 2012; Fraser et al. 2014; Lomax and Fraser
42
43
44 270 2015; Jardine et al. 2016; Jardine et al. 2017). As in pollen and spores, phenolic compounds
45
46 271 take on the role of UACs in cuticles, and these have shown to be preserved in Paleocene
47
48
49 272 *Ginkgo* cuticle (Blokker et al. 2006). Aromatic peaks are also present in FTIR spectra from a
50
51 273 range of fossil taxa analysed by Vajda et al. (2017), including specimens dating from the
52
53
54 274 latest Triassic. The relative importance of UV-B flux and taxonomy/phylogeny for
55
56 275 controlling cuticle chemistry will therefore need to be investigated, but there is scope for

276 cuticle chemistry to be developed as a palaeo-UV-B proxy, as has been the case with pollen
277 and spores (Blokker et al. 2006; de Leeuw et al. 2006; Rozema et al. 2009).

278

279 **Acknowledgements**

280 We thank Benjamin Bomfleur, Michael Krings and Christian Pott for the invitation to
281 contribute to this special issue of *PalZ*, and Hans Kerp for his many years of research into the
282 interpretation and use of cuticular remains. This research was supported by the
283 Palaeontological Association (PEJ: PA-RG201802) and the Natural Environment Research
284 Council (BHL, WTF, MK: NE/R001324/1; WTF: NE/P013724/1).

285

286 **References**

- 287 Abu Hamad, A., P. Blumenkemper, H. Kerp, and B. Bomfleur. 2017. *Dicroidium bandelii* sp.
288 nov. (corytospermalean foliage) from the Permian of Jordan. *Paläontologische*
289 *Zeitschrift* 91:641-648. doi:10.1007/s12542-017-0384-2.
- 290 Abu Hamad, A., H. Kerp, B. Vörding, and K. Bandel. 2008. A Late Permian flora with
291 *Dicroidium* from the Dead Sea region, Jordan. *Review of Palaeobotany and*
292 *Palynology* 149:85-130.
- 293 Blokker, P., P. Boelen, R. Broekman, and J. Rozema. 2006. The occurrence of *p*-coumaric
294 acid and ferulic acid in fossil plant materials and their use as UV-proxy. *Plant*
295 *Ecology* 182:197-207.
- 296 Blokker, P., D. Yeloff, P. Boelen, R.A. Broekman, and J. Rozema. 2005. Development of a
297 Proxy for Past Surface UV-B Irradiation: A Thermally Assisted Hydrolysis and
298 Methylation py-GC/MS Method for the Analysis of Pollen and Spores. *Analytical*
299 *Chemistry* 77:6026-6031.

- 300 Bomfleur, B., A.L. Decombeix, I.H. Escapa, A.B. Schwendemann, and B. Axsmith. 2013.
1
2 301 Whole-plant concept and environment reconstruction of a *Telemachus* conifer
3
4 302 (Voltziales) from the Triassic of Antarctica. *International Journal of Plant Sciences*
5
6
7 303 174 (3):425-444. doi:10.1086/668686.
- 8
9 304 D'Angelo, J.A. 2006. Analysis by Fourier transform infrared spectroscopy of *Johnstonia*
10
11 305 (Corytospermales, Corytospermaceae) cuticles and compressions from the Triassic
12
13
14 306 of Cacheuta, Mendoza, Argentina. *Ameghiniana* 43 (4):669-685.
- 15
16 307 D'Angelo, J.A., L.B. Escudero, W. Volkheimer, and E.L. Zodrow. 2011. Chemometric
17
18 308 analysis of functional groups in fossil remains of the *Dicroidium* flora (Cacheuta,
19
20
21 309 Mendoza, Argentina): Implications for kerogen formation. *International Journal of*
22
23
24 310 *Coal Geology* 87:97-111. doi:10.1016/j.coal.2011.05.005.
- 25
26 311 D'Angelo, J.A., and E.L. Zodrow. 2015. Chemometric study of structural groups in
27
28 312 medullosalean foliage (Carboniferous, fossil Lagerstätte, Canada): Chemotaxonomic
29
30
31 313 implications. *International Journal of Coal Geology* 138:42-54.
32
33
34 314 doi:10.1016/j.coal.2014.12.003.
- 35
36 315 D'Angelo, J.A., E.L. Zodrow, and A. Camargo. 2010. Chemometric study of functional
37
38 316 groups in Pennsylvanian gymnosperm plant organs (Sydney Coalfield, Canada):
39
40
41 317 Implications for chemotaxonomy and assessment of kerogen formation. *Organic*
42
43 318 *Geochemistry* 41:1312-1325. doi:10.1016/j.orggeochem.2010.09.010.
- 44
45 319 de Leeuw, J.W., G.J.M. Versteegh, and P.F. van Bergen. 2006. Biomacromolecules of algae
46
47 320 and plants and their fossil analogues. *Plant Ecology* 182:209-233.
48
49
50 321 doi:10.1007/s11258-005-9027-x.
- 51
52 322 Dell'Anna, R., P. Lazzeri, M. Frisanco, F. Monti, F. Malvezzi Campeggi, E. Gottardini, and
53
54
55 323 M. Bersani. 2009. Pollen discrimination and classification by Fourier transform
56
57
58
59
60
61
62
63
64
65

324 infrared (FT-IR) microspectroscopy and machine learning. *Analytical and*
1
2 325 *bioanalytical chemistry* 394 (5):1443-1452. doi:10.1007/s00216-009-2794-9.
3
4
5 326 Depciuch, Joanna, Idalia Kasprzyk, Elzbieta Drzymala, and Magdalena Parlinska-Wojtan.
6
7 327 2018. Identification of birch pollen species using FTIR spectroscopy. *Aerobiologia*.
8
9
10 328 doi:10.1007/s10453-018-9528-4.
11
12 329 Diefendorf, A. F., K. E. Mueller, S. L. Wing, P. L. Koch, and K. H. Freeman. 2010. Global
13
14 330 patterns in leaf ^{13}C discrimination and implications for studies of past and future
15
16 331 climate. *Proceedings of the National Academy of Sciences USA* 107 (13):5738-5743.
17
18
19 332 doi:10.1073/pnas.0910513107.
20
21
22 333 Dominguez, E., M. D. Fernandez, J. C. Hernandez, J. P. Parra, L. Espana, A. Heredia, and J.
23
24 334 Cuartero. 2012. Tomato fruit continues growing while ripening, affecting cuticle
25
26 335 properties and cracking. *Physiologia Plantarum* 146 (4):473-486. doi:10.1111/j.1399-
27
28 3054.2012.01647.x.
29 336
30
31 337 Dominguez, E., J. A. Heredia-Guerrero, and A. Heredia. 2017. The plant cuticle: old
32
33
34 338 challenges, new perspectives. *J Exp Bot* 68 (19):5251-5255. doi:10.1093/jxb/erx389.
35
36 339 Domínguez, E., J.A. Heredia-Guerrero, and A. Heredia. 2011. The biophysical design of
37
38
39 340 plant cuticles: an overview. *New Phytologist* 189:938-949. doi:10.1111/j.1469-
40
41 341 8137.2010.03553.x.
42
43
44 342 Esler, M.B., D.W.T. Griffith, S.R. Wilson, and L.P. Steele. 2000. Precision Trace Gas
45
46 343 Analysis by FT-IR Spectroscopy. 2. The $^{13}\text{C}/^{12}\text{C}$ Isotope Ratio of CO_2 . *Analytical*
47
48 344 *Chemistry* 72:216-221.
49
50
51 345 Foster, G.L., D.L. Royer, and D.J. Lunt. 2017. Future climate forcing potentially without
52
53 346 precedent in the last 420 million years. *Nature Communications* 8 (14845).
54
55
56 347 doi:10.1038/ncomms14845.
57
58
59
60
61
62
63
64
65

- 348 Fraser, W.T., B.H. Lomax, P.E. Jardine, W.D. Gosling, and M.A. Sephton. 2014. Pollen and
1
2 349 spores as a passive monitor of ultraviolet radiation. *Frontiers in Ecology and*
3
4
5 350 *Evolution* 2. doi:10.3389/fevo.2014.00012.
6
- 7 351 Fraser, W.T., M.A. Sephton, J.S. Watson, S. Self, B.H. Lomax, D.I. James, C.H. Wellman,
8
9
10 352 T.V. Callaghan, and D.J. Beerling. 2011. UV-B absorbing pigments in spores:
11
12 353 biochemical responses to shade in a high-latitude birch forest and implications for
13
14 354 sporopollenin-based proxies of past environmental change. *Polar Research* 30:8312.
15
16
17 355 doi:10.3402/polar.v30i0.8312.
18
- 19 356 Gill, F. L., J. Hummel, A. R. Sharifi, A. P. Lee, and B. H. Lomax. 2018. Diets of giants: the
20
21
22 357 nutritional value of sauropod diet during the Mesozoic. *Palaeontology* 61 (5):647-
23
24 358 658. doi:10.1111/pala.12385.
25
- 26 359 Gonzalez, J. A., M. G. Gallardo, C. Boero, M.L. Cruz, and F. E. Prado. 2007. Altitudinal and
27
28
29 360 seasonal variation of protective and photosynthetic pigments in leaves of the world's
30
31
32 361 highest elevation trees *Polylepis tarapacana* (Rosaceae). *Acta Oecologica* 32:36-41.
33
- 34 362 Gupta, N.S. 2014. *Biopolymers: a molecular paleontology approach*. Topics in Geobiology,
35
36 363 vol. 38. Dordrecht: Springer.
37
- 38
39 364 Gupta, N.S., D.E.G. Briggs, M.E. Collinson, R.P. Evershed, R. Michels, K.S. Jack, and R.D.
40
41 365 Pancost. 2007a. Evidence for the in situ polymerisation of labile aliphatic organic
42
43 366 compounds during the preservation of fossil leaves: Implications for organic matter
44
45
46 367 preservation. *Organic Geochemistry* 38:499-522.
47
48
49 368 doi:10.1016/j.orggeochem.2006.06.011.
50
- 51 369 Gupta, N.S., R. Michels, D.E.G. Briggs, M.E. Collinson, R.P. Evershed, and R.D. Pancost.
52
53
54 370 2007b. Experimental evidence for the formation of geomacromolecules from plant
55
56 371 leaf lipids. *Organic Geochemistry* 38 (1):28-36.
57
58 372 doi:10.1016/j.orggeochem.2006.09.014.
59
60
61
62
63
64
65

- 373 Heredia-Guerrero, J. A., J. J. Benitez, E. Dominguez, I. S. Bayer, R. Cingolani, A.
1
2 374 Athanassiou, and A. Heredia. 2014. Infrared and Raman spectroscopic features of
3
4
5 375 plant cuticles: a review. *Frontiers in Plant Sciences* 5:305.
6
7 376 doi:10.3389/fpls.2014.00305.
8
9
10 377 Jardine, P. E., F.A.J. Abernethy, B. H. Lomax, W. D. Gosling, and W. T. Fraser. 2017.
11
12 378 Shedding light on sporopollenin chemistry, with reference to UV reconstructions.
13
14 379 *Review of Palaeobotany and Palynology* 238:1-6.
15
16
17 380 doi:10.1016/j.revpalbo.2016.11.014.
18
19 381 Jardine, P. E., W. T. Fraser, B. H. Lomax, M. A. Sephton, T. M. Shanahan, C.S. Miller, and
20
21
22 382 W. D. Gosling. 2016. Pollen and spores as biological recorders of past ultraviolet
23
24 383 irradiance. *Scientific Reports* 6 (39269):1-8. doi:10.1038/srep39269.
25
26
27 384 Julier, A.C.M., P.E. Jardine, A.L. Coe, W.D. Gosling, B.H. Lomax, and W.T. Fraser. 2016.
28
29 385 Chemotaxonomy as a tool for interpreting the cryptic diversity of Poaceae pollen.
30
31 386 *Review of Palaeobotany and Palynology* 235:140-147.
32
33
34 387 Kerp, H. 1990. The study of fossil gymnosperms by means of cuticular analysis. *Palaios*
35
36 388 5:548-569.
37
38
39 389 Kerp, H., A. Abu Hamad, B. Vörding, and K. Bandel. 2006. Typical Triassic Gondwanan
40
41 390 floral elements in the Upper Permian of the paleotropics. *Geology* 34 (4):265-268.
42
43 391 doi:10.1130/G22187.1.
44
45
46 392 Liland, K.H., and B-H. Mevik. 2015. baseline: Baseline Correction of Spectra.
47
48
49 393 Lomax, B.H., and W.T. Fraser. 2015. Palaeoproxies: Botanical monitors and recorders of
50
51 394 atmospheric change. *Palaeontology* 58 (5):759-768. doi:doi: 10.1111/pala.12180.
52
53
54 395 Lomax, B.H., J. Hilton, R.M. Bateman, G.R. Upchurch, J.A. Lake, I.J. Leitch, A. Cromwell,
55
56 396 and C.A. Knight. 2014. Reconstructing relative genome size of vascular plants
57
58 397 through geological time. *New Phytologist* 201 (2):636-644.
59
60
61
62
63
64
65

- 398 Lomax, B.H., W.T. Fraser, G. Harrington, S. Blackmore, M.A. Sephton, and N.B.W. Harris.
1
2 399 2012. A novel palaeoaltimetry proxy based on spore and pollen wall chemistry. *Earth*
3
4
5 400 *and Planetary Science Letters* 353-354:22-28. doi:10.1016/j.epsl.2012.07.039.
6
- 7 401 Lomax, B.H., W.T. Fraser, M.A. Sephton, T.V. Callaghan, S. Self, M. Harfoot, J.A. Pyle,
8
9
10 402 C.H. Wellman, and D.J. Beerling. 2008. Plant spore walls as a record of long-term
11
12 403 changes in ultraviolet-B radiation. *Nature Geoscience* 1 (9):592-596.
13
14 404 doi:10.1038/ngeo278.
15
- 16
17 405 Lyons, P.L., W.H. Orem, M. Mastalerz, E.L. Zodrow, A. Vieth-Redemann, and R.M. Bustin.
18
19 406 1995. ¹³C NMR, micro-FTIR and fluorescence spectra, and pyrolysis-gas
20
21 407 chromatograms of coalified foliage of late Carboniferous medullosan seed ferns,
22
23
24 408 Nova Scotia, Canada: Implications for coalification and chemotaxonomy.
25
26 409 *International Journal of Coal Geology* 27:227-248.
27
28
- 29 410 McElwain, J. C., and M. Steinthorsdottir. 2017. Paleoecology, Ploidy, Paleoatmospheric
30
31 411 Composition, and Developmental Biology: A Review of the Multiple Uses of Fossil
32
33
34 412 Stomata. *Plant Physiology* 174 (2):650-664. doi:10.1104/pp.17.00204.
35
- 36 413 McElwain, J.C., and W.G. Chaloner. 1995. Stomatal density and index of fossil plants track
37
38
39 414 atmospheric carbon dioxide in the Palaeozoic. *Annals of Botany* 76:389-395.
40
- 41 415 Möhle, B., M.E. Collinson, P.F. Finch, B.A. Stankiewicz, A.C. Scott, and R. Wilson. 1998.
42
43 416 Factors influencing the preservation of plant cuticles: a comparison of morphology
44
45
46 417 and chemical composition of modern and fossil examples. *Organic Geochemistry* 29
47
48 418 (5-7):1369-1380.
49
50
- 51 419 Möhle, B., M.E. Collinson, A.C. Scott, and P. Finch. 2002. Chemosystematic and
52
53 420 microstructural investigations on Carboniferous seed plant cuticles from four North
54
55
56 421 American localities. *Review of Palaeobotany and Palynology* 120:41-52.
57
58
59
60
61
62
63
64
65

- 1
2
3
4
5
6
7
8
9
10
11
12
13
14
15
16
17
18
19
20
21
22
23
24
25
26
27
28
29
30
31
32
33
34
35
36
37
38
39
40
41
42
43
44
45
46
47
48
49
50
51
52
53
54
55
56
57
58
59
60
61
62
63
64
65
- 422 Möсле, B., P. Finch, M.E. Collinson, and A.C. Scott. 1997. Comparison of modern and fossil
423 plant cuticles by selective chemical extraction monitored by flash pyrolysis-gas
424 chromatography-mass spectrometry and electron microscopy. *Journal of Analytical
425 and Applied Pyrolysis* 40-41:585-597.
- 426 Neitzke, M., and A. Therburg. 2003. Seasonal changes in UV-B absorption in beech leaves
427 (*Fagus sylvatica* L.) along an elevation gradient. *Forstwissenschaftliches Centralblatt*
428 122:1-21.
- 429 Olcott Marshall, A., and C.P. Marshall. 2014. Vibrational spectroscopy of fossils.
430 *Palaeontology* 58 (5):201-211. doi:10.1111/pala.12144.
- 431 Pappas, C.S., P.A. Tarantilis, P.C. Harizanis, and M.G. Polissiou. 2003. New Method for
432 Pollen Identification by FT-IR Spectroscopy. *Applied Spectroscopy* 57 (1):23-27.
- 433 Ramirez, F.J., P. Luque, A. Heredia, and M.J. Bukovac. 1992. Fourier Transform IR Study of
434 Enzymatically Isolated Tomato Fruit Cuticular Membrane. *Biopolymers* 32:1425-
435 1429.
- 436 R Core Team. 2017. R: A language and environment for statistical computing. Vienna,
437 Austria: R Foundation for Statistical Computing.
- 438 Renault, H., A. Alber, N. A. Horst, A. Basilio Lopes, E. A. Fich, L. Kriegshauser, G.
439 Wiedemann et al. 2017. A phenol-enriched cuticle is ancestral to lignin evolution in
440 land plants. *Nature Communications* 8:14713. doi:10.1038/ncomms14713.
- 441 Ribeiro da Luz, B. 2006. Attenuated total reflectance spectroscopy of plant leaves: a tool for
442 ecological and botanical studies. *New Phytologist* 172 (2):305-318.
443 doi:10.1111/j.1469-8137.2006.01823.x.
- 444 Richey, J.D., G.R. Upchurch, I.P. Montañez, B.H. Lomax, M.B. Suarez, N.M.J. Crout, R.M.
445 Joeckele, G.A. Ludvigson, and J.J. Smith. 2018. Changes in CO₂ during Ocean

- 446 Anoxic Event 1d indicate similarities to other carbon cycle perturbations. *Earth and*
1
2 447 *Planetary Science Letters* 491:172-182.
3
- 4
5 448 Rozema, J., P. Blokker, M. A. Mayoral Fuertes, and R. Broekman. 2009. UV-B absorbing
6
7 449 compounds in present-day and fossil pollen, spores, cuticles, seed coats and wood:
8
9
10 450 evaluation of a proxy for solar UV radiation. *Photochemical & photobiological*
11
12 451 *sciences : Official journal of the European Photochemistry Association and the*
13
14 452 *European Society for Photobiology* 8 (9):1233-1243. doi:10.1039/b904515e.
15
- 16
17 453 Rozema, J., R.A. Broekman, P. Blokker, B. Meijkamp, N. de Bakker, J. van de Staaij, A. van
18
19 454 Beem, F. Ariese, and S.M. Kars. 2001a. UV-B absorbance and UV-B absorbing
20
21
22 455 compounds (*para*-coumaric acid) in pollen and sporopollenin: the perspective to track
23
24 456 historic UV-B levels. *Journal of Photochemistry and Photobiology B: Biology*
25
26 457 62:108-117.
27
- 28
29 458 Rozema, J., A.J. Noordjik, R.A. Broekman, A. van Beem, B.M. Meijkamp, N.V.J. de Bakker,
30
31 459 J.W.M. van de Staaij et al. 2001b. (Poly)phenolic compounds in pollen and spores of
32
33
34 460 Antarctic plants as indicators of UV-B: A new proxy for the reconstruction of past
35
36 461 solar UV-B? *Plant Ecology* 154:11-26.
37
- 38
39 462 Rozema, J., J. van de Staaij, L-O. Björn, and N de Bakker. 1999. Depletion of stratospheric
40
41 463 ozone and solar UV-B radiation: Evolution of land plants, UV-screens and functions
42
43 464 of polyphenolics. In *Stratospheric ozone depletion: The effects of enhanced UV-B*
44
45 465 *radiation on terrestrial ecosystems*, ed. J. Rozema, 1-19. Leiden: Backhuys.
46
47
- 48
49 466 Salminen, T. A., D. M. Eklund, V. Joly, K. Blomqvist, D. P. Matton, and J. Edqvist. 2018.
50
51 467 Deciphering the Evolution and Development of the Cuticle by Studying Lipid
52
53 468 Transfer Proteins in Mosses and Liverworts. *Plants* 7 (1). doi:10.3390/plants7010006.
54
55
- 56 469 Steinthorsdottir, M., C. Elliott-Kingston, and K.L. Bacon. 2018. Cuticle surfaces of fossil
57
58 470 plants as a potential proxy for volcanic SO₂ emissions: observations from the
59
60
61
62
63
64
65

- 471 Triassic–Jurassic transition of East Greenland. *Palaeobiodiversity and*
1
2 472 *Palaeoenvironments* 98:49. doi:10.1007/s12549-017-0297-9.
3
4
5 473 Stevens, A., and L. Ramirez-Lopez. 2013. An introduction to the prospectr package. *R*
6
7 474 *package Vignette* R package version 0.1.3.
8
9
10 475 Tegelaar, E.W., J. Wattendorff, and J.W. de Leeuw. 1993. Possible effects of chemical
11
12 476 heterogeneity in higher land plant cuticles on the preservation of its ultrastructure
13
14 477 upon fossilization. *Review of Palaeobotany and Palynology* 77:149-170.
15
16
17 478 Vajda, V., M. Pucetaite, S. McLoughlin, A. Engdahl, J. Heimdal, and P. Uvdal. 2017.
18
19 479 Molecular signatures of fossil leaves provide unexpected new evidence for extinct
20
21 480 plant relationships. *Nature Ecology and Evolution* 1 (8):1093-1099.
22
23
24 481 doi:10.1038/s41559-017-0224-5.
25
26
27 482 Villena, J.F., E. Domínguez, and A. Heredia. 2000. Monitoring Biopolymers Present in Plant
28
29 483 Cuticles by FT-IR Spectroscopy. *Journal of Plant Physiology* 156:419-422.
30
31 484 doi:10.1016/S0176-1617(00)80083-8.
32
33
34 485 Watson, J.S., M.A. Sephton, S.V. Sephton, S. Self, W.T. Fraser, B.H. Lomax, I. Gilmour,
35
36 486 C.H. Wellman, and D.J Beerling. 2007. Rapid determination of spore chemistry using
37
38 487 thermochemolysis gas chromatography-mass spectrometry and micro-Fourier
39
40 488 transform infrared spectroscopy. *Photochemical and Photobiological Sciences* 6:689-
41
42 489 694. doi:10.1039/b617794h.
43
44
45
46 490 Willis, K. J., A. Feurdean, H. J. B. Birks, A. E. Bjune, E. Breman, R. Broekman, J. A.
47
48 491 Grytnes, M. New, J. S. Singarayer, and J. Rozema. 2011. Quantification of UV-B flux
49
50 492 through time using UV-B-absorbing compounds contained in fossil *Pinus*
51
52 493 sporopollenin. *New Phytologist* 192 (2):553-560. doi:10.1111/j.1469-
53
54 494 8137.2011.03815.x.
55
56
57
58
59
60
61
62
63
64
65

- 1
2
3
4
5
6
7
8
9
10
11
12
13
14
15
16
17
18
19
20
21
22
23
24
25
26
27
28
29
30
31
32
33
34
35
36
37
38
39
40
41
42
43
44
45
46
47
48
49
50
51
52
53
54
55
56
57
58
59
60
61
62
63
64
65
- 495 Woodward, F.I. . 1987. Stomatal numbers are sensitive to increases in CO₂ from pre-
496 industrial levels. *Nature* 327:617-618.
- 497 Zhiyan, Z., and W. Xiangwu. 2006. The rise of ginkgoalean plants in the early Mesozoic: a
498 data analysis. *Geological Journal* 41:363-375. doi:10.1002/gj.1049.
- 499 Zimmermann, B., and A. Kohler. 2014. Infrared spectroscopy of pollen identifies plant
500 species and genus as well as environmental conditions. *Plos One* 9 (4):1-12.
501 doi:10.1371/journal.pone.0095417.t001.
- 502 Zimmermann, B., V. Tafintseva, M. Balu, M. Høegh Berdahl, and A. Kohler. 2016.
503 Analysis of Allergenic Pollen by FTIR Microspectroscopy. *Analytical Chemistry*
504 88:803-811. doi:10.1021/acs.analchem.5b03208.
- 505 Zodrow, E.L., J.A. D'Angelo, R. Helleur, and Z. Simunek. 2012a. Functional groups and
506 common pyrolysate products of *Odontopteris cantabrica* (index fossil for the
507 Cantabrian Substage, Carboniferous). *International Journal of Coal Geology* 100:40-
508 50. doi:10.1016/j.coal.2012.06.002.
- 509 Zodrow, E.L., J.A. D'Angelo, M. Mastalerz, and D. Keefe. 2009. Compression–cuticle
510 relationship of seed ferns: Insights from liquid–solid states FTIR (Late Palaeozoic–
511 Early Mesozoic, Canada–Spain–Argentina). *International Journal of Coal Geology*
512 79:61-73. doi:10.1016/j.coal.2009.06.001.
- 513 Zodrow, E.L., J.A. D'Angelo, W.A. Taylor, T. Catelani, J. A. Heredia-Guerrero, and M.
514 Mastalerz. 2016. Secretory organs: Implications for lipid taxonomy and kerogen
515 formation (seed ferns, Pennsylvanian, Canada). *International Journal of Coal*
516 *Geology* 167:184-200. doi:10.1016/j.coal.2016.10.004.
- 517 Zodrow, E.L., and M. Mastalerz. 2001. Chemotaxonomy for naturally macerated tree-fern
518 cuticles (Medullosales and Marattiales), Carboniferous Sydney and Mabou Sub-
519 Basins, Nova Scotia, Canada. *International Journal of Coal Geology* 47:255-275.

- 520 Zodrow, E.L., and M. Mastalerz. 2002. FTIR and py-GC-MS spectra of true-fern and seed-
1 fern sphenopterids (Sydney Coalfield, Nova Scotia, Canada, Pennsylvanian).
2 521
3
4
5 522 *International Journal of Coal Geology* 51:111-127.
6
7 523 Zodrow, E.L., and M. Mastalerz. 2009. A proposed origin for fossilized Pennsylvanian plant
8
9
10 524 cuticles by pyrite oxidation (Sydney Coalfield, Nova Scotia, Canada). *Bulletin of*
11
12 525 *Geosciences* 84 (2):227-240. doi:10.3140/bull.geosci.1094.
13
14 526 Zodrow, E.L., M. Mastalerz, and R. Helleur. 2012b. *Lepidodendron dawsonii*: functional
15
16
17 527 groups and pyrolysates of compression and fossilized-cuticle (Late Asturian, Canada).
18
19 528 *Geologica Croatica* 65 (3):367-374.
20
21 529 Zodrow, E.L., M. Mastalerz, W.H. Orem, Z. Simunek, and A.R. Bashforth. 2000. Functional
22
23
24 530 groups and elemental analyses of cuticular morphotypes of *Cordaites principalis*
25
26
27 531 (Germar) Geinitz, Carboniferous Maritimes Basin, Canada. *International Journal of*
28
29 532 *Coal Geology* 45:1-19.
30

31 533

32 534

535 **Table 1** IR absorbance peaks measured from the *Ginkgo* cuticles, shown in Figs. 5 and S2.

536 Peak heights were measured as the maximum absorbance value within the given

537 measurement range. Peak assignments and cuticle component interpretations are from

538 Heredia-Guerrero et al. (2014). ν = stretching, δ = bending, a = asymmetric, s = symmetric

Assignment	Peak position (cm ⁻¹)	Measurement range (cm ⁻¹)	Cuticle component
$\nu_a(\text{CH}_2)$	2920	2900 - 2940	Cutin, waxes
$\nu_s(\text{CH}_2)$	2850	2830 - 2870	Cutin, waxes
$\nu(\text{C=O})$ ester	1710	1695 - 1720	Cutin
$\nu(\text{C-C})$ aromatic	1600	1595 - 1615	Phenolic compounds
$\nu(\text{C-C})$ aromatic (conjugated with C=C)	1515	1505 - 1525	Phenolic compounds
$\delta(\text{CH}_2)$	1460	1450 - 1470	Cutin, waxes
$\nu_a(\text{C-O-C})$ ester	1167	1155 - 1180	Cutin
$\nu(\text{C-O})$	1020	1010 - 1030	Polysaccharides

539

540 **Figures**

1
2 541 **Fig 1** Atmospheric CO₂ (ppm) and changes in ginkgoalean diversity through time. CO₂ data
3
4
5 542 are the Foster et al. (2017) LOESS compilation based on literature data assembled by
6
7 543 integrating five independent proxies (stomata, pedogenic $\delta^{13}\text{C}$, liverwort $\delta^{13}\text{C}$, foraminiferal
8
9
10 544 $\delta^{11}\text{B}$ and alkenone $\delta^{13}\text{C}$). See SOM of Foster et al. (2017) for full details. Ginkgoalean
11
12 545 diversity is taken from Figure 1 of Zhiyan and Xiangwu (2006) and refers to the number of
13
14
15 546 genera/ morphogenera as recorded by the presence of vegetative organs

16
17 547
18
19 548 **Fig 2** Mean ATR-FTIR spectrum for the 400 ppm abaxial cuticles, showing the main peaks
20
21
22 549 mentioned in the text

23
24
25 550
26
27 551 **Fig 3** Mean ATR-FTIR spectrum for each CO₂ treatment by leaf surface combination

28
29 552
30
31
32 553 **Fig 4** Principal Component Analysis (PCA) plots for *Ginkgo* leaf cuticle ATR-FTIR data. **a**
33
34 554 and **e** PCA axes 1 versus 2, and 3 versus 4, respectively. Values in parentheses are the
35
36
37 555 percentage of variance in the data explained by each PCA axis. **b**, **c**, **e** and **f** Loadings plots
38
39 556 for the PCA axes

40
41 557
42
43
44 558 **Fig 5** Heights of selected IR absorbance peaks grouped by CO₂ treatment, for the <3100 cm⁻¹
45
46 559 spectra. Abaxial cuticle data are shown as boxplots, where the thick horizontal line denotes
47
48
49 560 the median value, the edges of the box the upper and lower quartiles, and the whiskers the
50
51 561 extremes of the data, up to a limit of 1.5 times the interquartile range (values beyond this are
52
53
54 562 shown as individual circles. Adaxial cuticle data are shown as grey diamonds. See Fig. S2 for
55
56 563 peak heights measured from the <1800 cm⁻¹ data

Figure 1

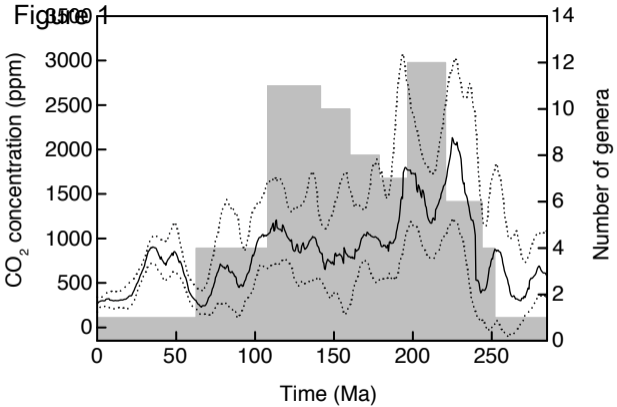


Figure 2

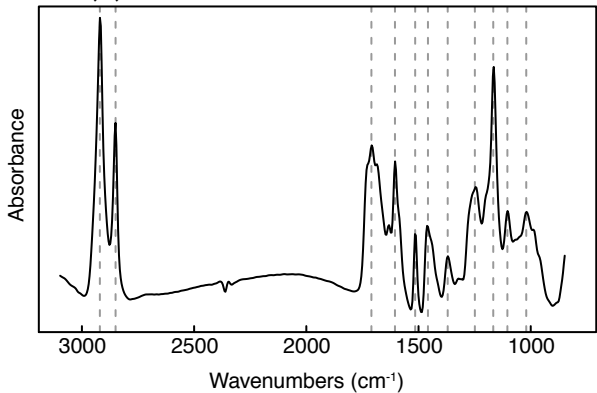


Figure 3

Abaxial cuticles

Adaxial cuticles

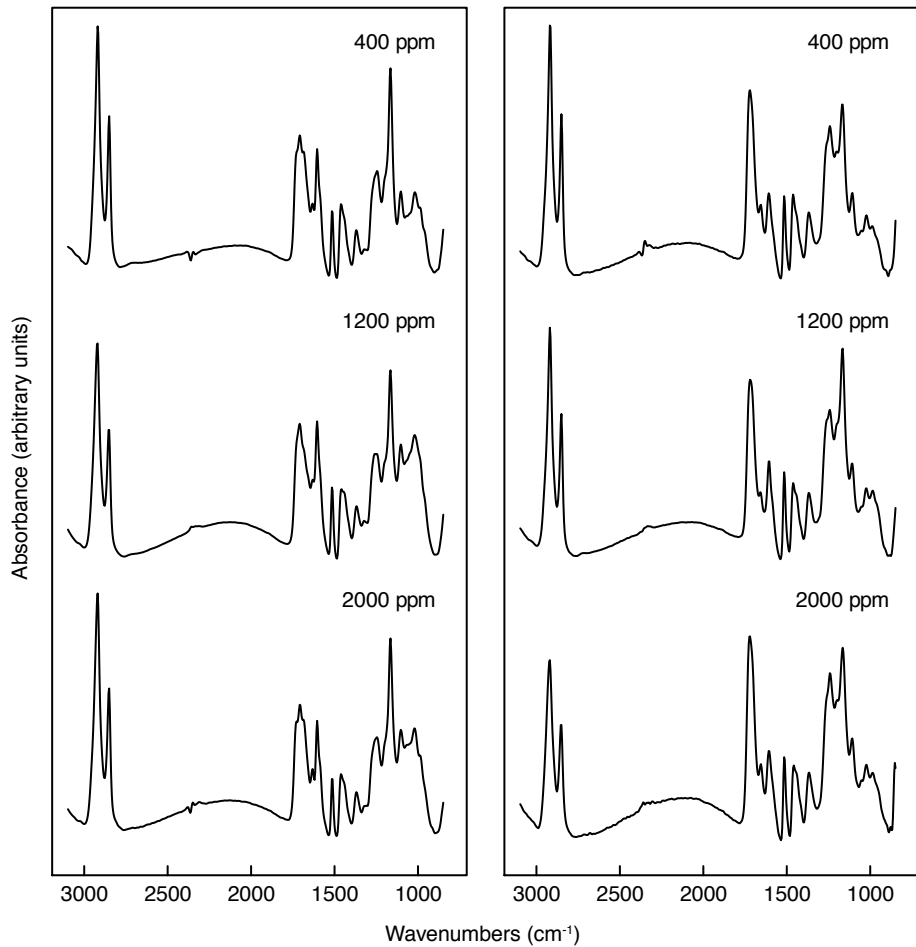


Figure 4

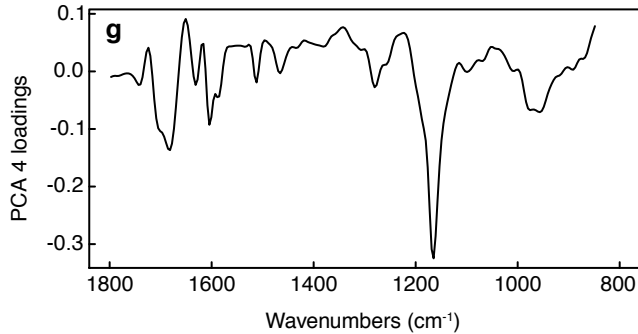
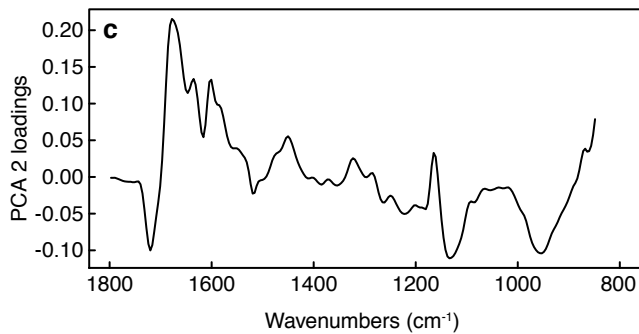
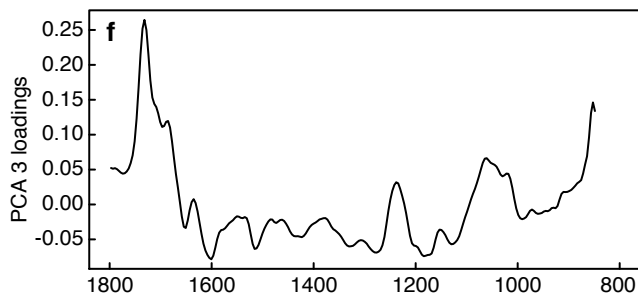
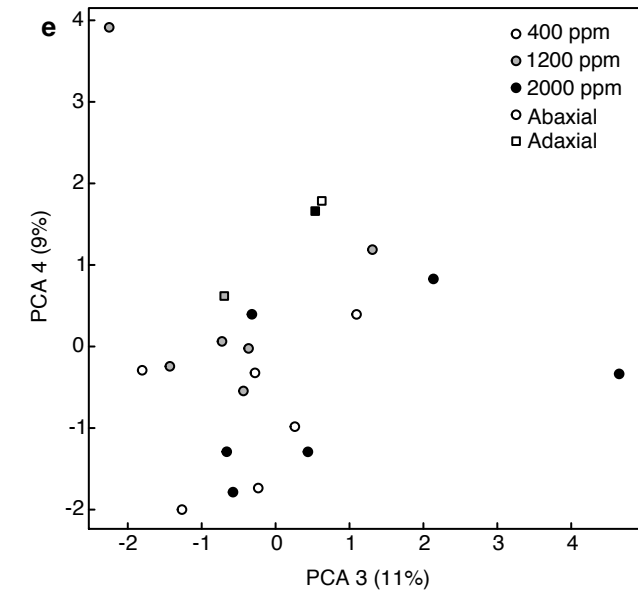
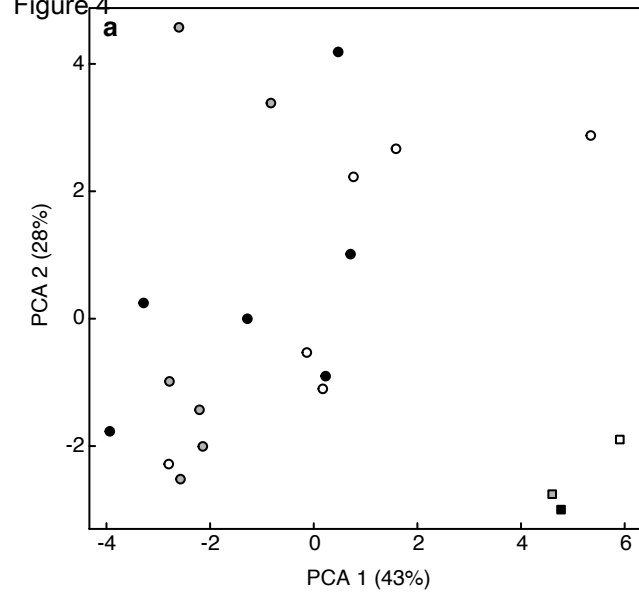
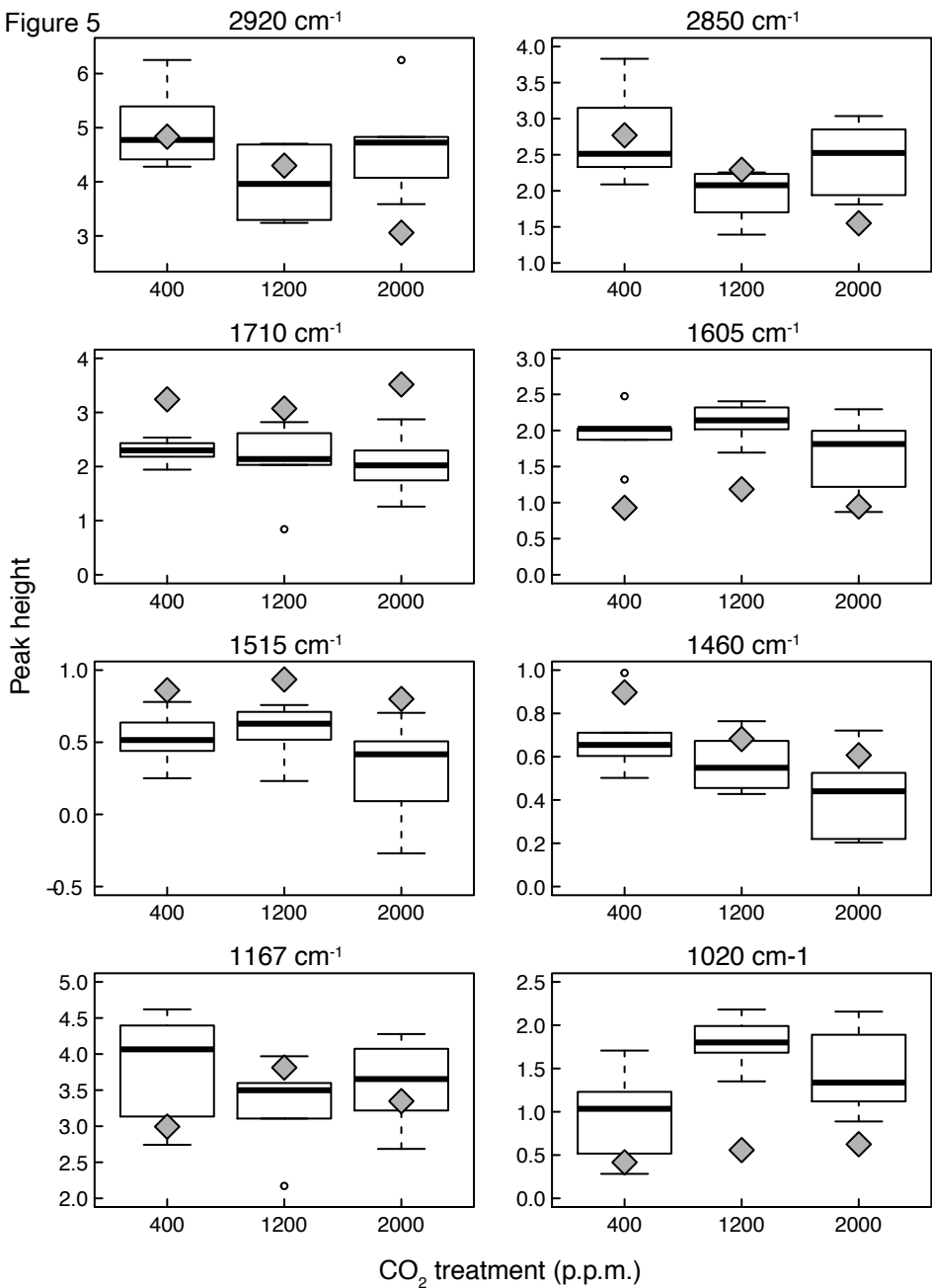


Figure 5

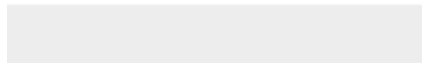




[Click here to access/download](#)

Supplementary Material

[JardineEtAl_GinkgoCuticleCO2_SI_Figs.pdf](#)





[Click here to access/download](#)

Supplementary Material

JardineEtAl_GinkgoCuticleCO2_Data.xlsx

